Journal of Computational Science 21 (2017) 223–231

Contents lists available at ScienceDirect

Journal of Computational Science

journal homepage: www.elsevier.com/locate/jocs

Segmentation of prostate contours for automated diagnosis using ultrasound images: A survey

Raman Preet Singh [a,*], Savita Gupta [a], U. Rajendra Acharya [b,c,d,e]

[a] Department of Computer Science and Engineering, UIET, Panjab University, 160014, India
[b] Department of Electronics and Computer Engineering, Ngee Ann Polytechnic, 599489, Singapore
[c] Department of Biomedical Engineering, School of Science and Technology, SIM University, 599491, Singapore
[d] Department of Biomedical Engineering, Faculty of Engineering, University of Malaya, 50603, Malaysia
[e] School of Engineering, Singapore Institute of Technology-Glasgow, Singapore

ARTICLE INFO

Article history:
Received 12 March 2017
Received in revised form 20 April 2017
Accepted 26 April 2017
Available online 29 April 2017

Keywords:
B-mode Transrectal ultrasound image (TRUS)
Segmentation
Feature extraction
Brachytherapy
Prostate

ABSTRACT

Prostate cancer is the most common cancer that affects elderly men. The conventional non-imaging screening test for prostate cancer like prostate antigen (PSA) and digital rectal examination (DRE) tests generally lack specificity. Ultrasound is the most commonly available, inexpensive, non-invasive, and radiation-free imaging modality among all the screening imaging modalities available for prostate cancer diagnosis. The precise segmentation of prostate contours in ultrasound images is crucial in applications such as the exact placement of needles during biopsies, computing the prostate gland volume, and to localize the prostate cancer. Moreover, the low-dose-rate (LDR) brachytherapy treatment in which radioactive seeds are implanted in the prostate region requires accurate contouring of the prostate gland in ultrasound images. Therefore, it is very important to segment the prostrate region accurately for the diagnosis and treatment. This paper aims to present the analysis of existing approaches used for the segmentation of prostate in transrectal ultrasound (TRUS) images. In this survey, different segmentation methods used to extract the prostrate using criteria such as mean absolute distance, Hausdorff distance and time are discussed in detail and compared.

1. Introduction

After skin cancer, prostate cancer is the most common cancer in USA. According to American cancer society, there are about 180,890 new cases and 26,120 deaths due to prostate cancer in 2016 [1]. Prostate disease can be classified in to *three* categories: prostatitis, benign prostatic hyperplasia (BHP), and adenocarcinoma [2]. Prostatitis is an inflammation, usually caused by bacteria and can be cured by antibiotics. The BHP is due to the enlargement of prostate and requires surgery in the advanced stage. The adenocarcinoma is the cancerous state of the prostate and if not detected in an early stage, cancer spreads to other organs like bones, seminal vesicles and rectum. Hence, early detection of prostate cancer can significantly reduce the chances of death. The initial diagnosis of prostate cancer includes non-imaging tests such as digital rectal examination [3] and prostate specific antigen lack specificity [4]. These tests are used along with the medical imaging tests such as transrectal ultrasound (TRUS), magnetic resonance imaging (MRI) and computed tomography (CT) scan of prostate [5]. The variation in cellular density can be examined using MRI [6]. Increase in local perfusion can be studied with contrast enhanced computed tomography or MRI [12]. Ultrasound images are most commonly used for screening, as they are inexpensive in comparison with other medical imaging modalities, easy to use, and have no side effects. The ultrasound images are not inferior to MRI or CT images in terms of diagnostic importance [40].

Segmentation in ultrasound modality is highly dependent on the nature of data. Prostate ultrasound images contain high speckle noise, shadow artifacts due to calcification in prostate region, short range of gray levels and boundaries are missing especially at the base and apex region of the prostate [13], which makes the segmentation process difficult. However, ultrasound images are widely used in various computer aided diagnosis (CAD) systems [2,7–11], image guided interventions, and various therapies like brachytherapy. In localized prostate cancer, low-dose-rate (LDR) brachytherapy can be used to provide a quick and accurate diagnosis [14]. The brachytherapy implants small radioactive seeds inside the prostate gland. But before the implantation, volume and

* Corresponding author.
E-mail address: aru@np.edu.sg (R.P. Singh).

http://dx.doi.org/10.1016/j.jocs.2017.04.016
1877-7503/

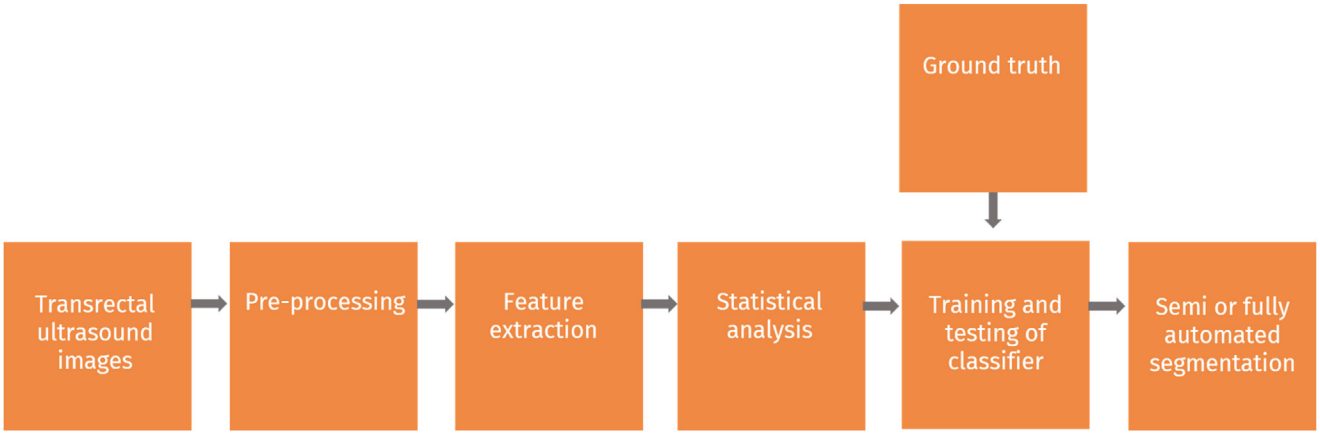

Fig. 1. Block diagram of texture-based prostate segmentation process in TRUS.

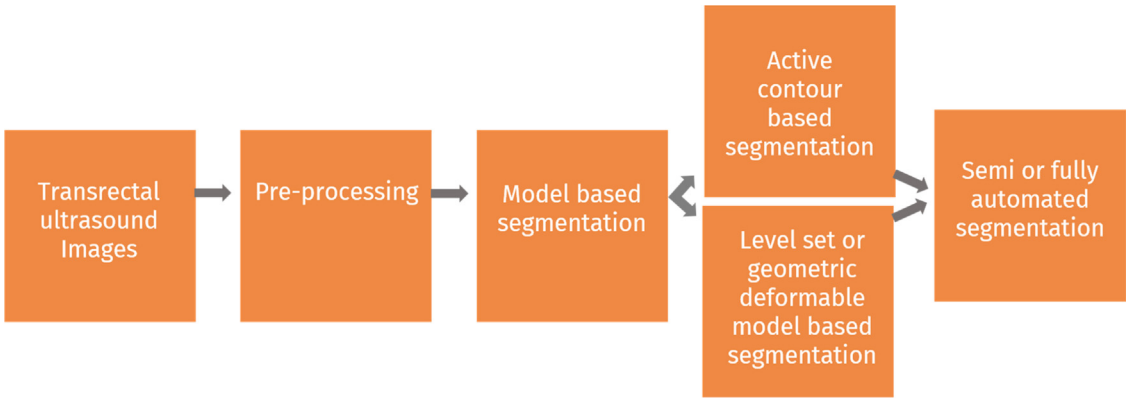

Fig. 2. Block diagram of model-based prostate segmentation process in TRUS.

shape of the prostate region is to be estimated. Therefore, it is very important to segment the prostate from TRUS image accurately. The shape and volume of the prostate is crucial for the diagnosis of prostate cancer [15]. In most of the clinical practice, manual or semi-automated segmentation is performed which is prone to observer variability due to the poor visibility of prostate in ultrasound images [16]. Moreover, the size and shape of the prostate is not fixed, as it changes because of bladder and rectum filling, cancer evolution rate and the effect of anesthesia. Hence, there is high requirement of the real time prostate delineation in clinical applications like brachytherapy where the decisions are made in the operating environment instantly before implantation of seeds [17].

Generally, ultrasound data is of two types (i) B-mode images and (ii) radio frequency (RF) signals. The B-mode ultrasound images are obtained by post-processing of RF signals captured from the transducer. Researchers have shown that there is significant amount of loss of information during this post-processing, which may be useful for classification of prostate region as cancerous or non-cancerous [18]. However, the conventional B-mode images are helpful in segmenting the prostate region. The texture-based and model-based procedures for prostate segmentation in TRUS images are depicted in Figs. 1 and 2 respectively. As TRUS images have low signal-to-noise ratio, speckle noise, and a very large number of edge features which are not a part of prostate contour. Therefore, a pre-processing is required to smooth the image while preserving the edge information [64–66].

Feature extraction is a crucial step in segmentation process. The major challenge is to extract the most relevant features from the input dataset. Statistical analysis is needed to select the subset of relevant features in model construction. The selected feature sets are used to train the classifier with known training parameters. Model validation techniques like k-fold cross validation, leave-one-out cross validation can be used to validate the final outcome with respect to the ground truth available [68]. As depicted in Fig. 2, Model based segmentation can be either active contour or geometric deformable model based segmentation technique.

In this paper, the primary focus is on the techniques developed for prostate segmentation in TRUS images. The segmentation of prostate from TRUS is important in various stages of clinical decision making process. For example prostate gland segmentation is helpful in determining the volume of the prostate, which aids in brachytherapy and treatment of BHP. Moreover, the prostate boundary obtained from the segmentation process helps in image fusion with other modalities like magnetic resonance imaging and radio frequency data to localize the cancer. Manual contouring of prostate is a difficult task and prone to inter and intra observer variability. Hence, the computer aided semiautomatic or fully automated segmentation techniques are investigated in this paper.

Earlier, Ghose et al. [19] carried out a survey on segmentation of prostate in multiple modalities like TRUS, MR, and CT images. Nobel et al. [20] considered various types of tissues like breast, heart, and prostate in their survey and techniques for vascular disorder are also examined. Zhu et al. [21] published the survey not only focusing on the segmentation of prostate, but also on the classification of ultrasound and MR images in cancerous and non-cancerous, staging of cancer and registration of ultrasound and MR images. Hence the surveys [19–21] consider wider spectrum. Shao et al. [22] proposed a survey primarily based on the prostate region detection in ultrasound images. Although the survey reported good classi-

fication of segmentation techniques, but the precise comparison catalogue is missing for the better comparative analysis. Moreover, there has been significant improvement in the prostate segmentation techniques over the past decade with more focus on the development of fully-automated segmentation techniques which can be used in real time. Therefore, in this paper, we have provided an up-to-date, substantial categorization and comparative analysis of prostate segmentation approaches defined for B-mode TRUS images. Both 2D and 3D TRUS images are covered in this survey.

This paper is structured in five sections with Section 2 concisely representing the prostate ultrasound image enhancement, analysis, and challenges associated with them. The different classes of prostate segmentation approaches, brief description of related papers, Advantages and limitations of various model-based segmentation techniques are discussed in Section 3. The various validation techniques used for the segmentation are described in Section 4. The critical analysis and discussion of various methods are provided in Section 5. Finally, the conclusion and future trends are presented in Section 6.

2. Image enhancement

A number of techniques [43–53] have been proposed for segmentation of prostate region from TRUS images and noise removal in ultrasound images. But the literature merely on enhancing the visual appearance of the prostate in TRUS images is limited. In some literature, Bayesian decision theory and stick algorithm [23–25] is used to identify the most likely set of edges in the TRUS image. Pathak et al. [25] used the concept of sticks to enhance the contrast of pubic arch in TRUS. Smaller stick size resulted in missing edges. As the stick length increased, detection of large scale linear features improved. However, large stick size resulted in more false edge detection. For the enhancement of ultrasound images, a number of researchers used wavelet based techniques [26–31], min-max filters [32], and Gaussian low pass filters [33]. Some of these techniques [26,32,33] have been tested on prostate ultrasound images. However, these methods do not yield much success due to excessive intensity variation in the prostate shape and low pass filtering blurred the prostate edges.

Ghose et al. [44] enhanced the texture information of prostate using various variants of local binary pattern (LBP) [69] and showed that, uniform LBP outperforms other variants of LBP as it produces a uniform prostate region that has different texture from its neighboring tissue. Therefore, uniform LBP significantly improves the visual appearance of prostate in TRUS. In order to reduce the speckle noise while preserving the edge information, Gupta et al. [64] proposed a method to despeckle the ultrasound image by combining the non-subsampled shear transform (NSST) with improved nonlinear diffusion equations (INDE). NSST and INDE significantly reduce the noise, preserve the edges and provide despeckled ultrasound image with good visual appearance. Gupta et al. [65] proposed a ripplet domain non-linear filtering approach to reduce the speckle noise. Ripplet transform is better than the other multiscale geometry analysis [66] due to its additional direction analysis property. Although the approaches [64,65] provided good visual experience of prostate in ultrasound images, there are number of challenges associated with the segmentation of prostate from ultrasound images as depicted in Fig. 3.

As depicted in Fig. 3 the thumb rule for segmenting prostate region is dark to grey transition in ultrasound image. However, Contouring the Prostate boundaries in ultrasound images is challenging due to (A) Low signal to noise ratio (SNR) value, B) texture is similar in prostate and non-prostate regions, and (C)boundary is not clearly visible due to shadow artifacts.

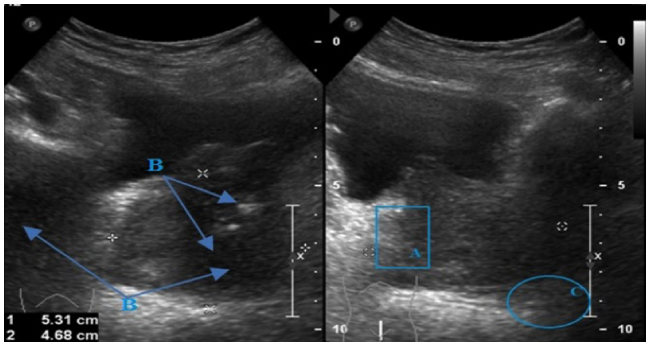

Fig. 3. Prostate ultrasound image describing different challenges in segmentation.

3. Categorization of prostate segmentation algorithms in ultrasound images

Segmentation in medical imaging plays a crucial role for volumetric and shape measurement of different tissues, feature extraction, surgery planning and analyzing the tissue in more meaningful and easier way. The number of segmentation techniques reported in texture based analysis [35–44] comes under region based segmentation approaches, model based techniques which includes shape priors based [44], deformable model, and super ellipse [16,46] based methods, semi-automated [40,41,45–47] or fully-automated methods [17,34,36,43,48–53]. Some other segmentation techniques are edge detection based, probability distribution based [59,60,73], and partial differential equation-based methods, which can be further divided in to parametric methods and level set methods [55–57].

3.1. Texture based approaches

Texture based approaches are dependent on the spatial arrangement of intensities or color in an image [42]. These approaches are further classified in structured and statistical approaches. Structured approaches deal with regularity in a pattern whereas statistical approaches consider an image as a quantitative calculation of intensities in an image.

Richard et al. [35] presented texture based automated segmentation method for 2D TRUS images by using *four* texture energy measures related to every pixel in the image. The algorithm is computationally intensive because its execution on quad core processor with 90 MHz speed took 16.87 min, which is not acceptable in clinical practice. Knollet al. [36] proposed a new technique for elastic deformation by localized multi scale boundary parameterization using one-dimensional wavelet transform. The wavelet transform parameterization is useful for the confined boundary shape analysis. This algorithm is tested on a dataset of 77 TRUS images. The volume difference (VD) and contour difference (CD) obtained between manual and algorithm generated boundary is 7.54% and 3.45 pixel respectively. Ladak et al. [37] reported a semi-automated segmentation technique for 2D TRUS images using model-based initialization and boundary is refined by discrete dynamic contour (DDC) in which a polyline is used for deformation. The average difference between manual and semi-automatically obtained contour is approximately 5 pixels with 90% accuracy.

Wang et al. [38] described *two* different techniques for three-dimensional ultrasound image segmentation of prostate boundary by slicing it into 2D images. Slices are obtained either in parallel or with rotational manner. The DDC approach is used until the boundary converges to actual prostate boundary. The *mean* absolute error of 5.4% and 1.7% is obtained for parallel and rotational approaches respectively. The algorithm tested on Pentium III, 700 MHz PC took

3 s to execute after optimization. This technique is fast and suitable for the clinical applications. However, the proposed technique suffers from error accumulation effect due to transmission of 2D contoured boundary in single slice to the nearby slice in which it is used as the initialization of the boundary.

Abolmaesumi et al. [39] proposed a new technique for segmenting prostate from 2D TRUS images by combining probabilistic data association filter with interacting multiple model. This combined technique is able to segment prostate with severe shadow. However, the algorithm is not robust with respect to the arbitrarily selected seed point. The seed point must see all the boundary points, which is not possible in the case due to the large intensity variation in prostate ultrasound images.

Shen et al. [40] presented a method for segmenting prostate using a dataset of eight ultrasound images at various different scales and orientations using statistical shape model. Image features are hierarchically represented by Gabor filter bank. Algorithm based segmentation is compared with the manual segmentation and the *mean* area error obtained is 1.66%. More accurate initialization approach could have been used to get more accurate results. Later, this work [40] is extended by Zhan et al. [41] by contouring of prostate from 3D TRUS images using statistical matching the texture and shape. Multiple Gabor-support vector machines are used to adaptively represent the texture priors. As two different regions of prostate have variable textures, adaptive classification of the prostate area is crucial.

Kachouie et al. [42] proposed texture-based segmentation on TRUS images using LBP. Generally, TRUS image for prostate possesses weak texture structure. However, LBP can be helpful in differentiating the prostate and non-prostate region based on texture properties.

Ding et al. [43] reduced the segmentation error by using continuity constraints and autoregressive model. Proposed algorithm is tested on 3D ultrasound images obtained from *nine* patients and the *mean* distance between automated segmentation and manual segmentation is 1.29 mm. Due to modified slicing approach, the effect of accumulation error is reduced in contrast with [38].

Ghose et al. [44] enhanced the texture properties of the TRUS image using LBP and appearance based statistical model is proposed to segment the prostate in a multi-resolution framework. The dice similarity coefficient (DSC) value 0.94 ± 0.01 is obtained and the average time of 0.6 ± 0.02 s is obtained for contouring the prostate, when tested on 70 TRUS images.

3.2. Model based approaches

Segmentation in 3D TRUS images is more challenging problem as compared to 2D TRUS image segmentation. In literature, Model based approaches were used for the 3D TRUS image data segmentation. These approaches are based on active contour models [58,62,71–74] (snakes or parametric deformable models), statistical model, and geometric deformable models (Level Sets) [22].

3.2.1. Active contour models

These models make use of the prior knowledge like structure, size, and position. These have the potential to contour the structure of an organism by utilizing restrictions obtained from the image data [62]. Deformable models utilize the curves (e.g. ellipsoids, superellipses), which advances under the impact of internal and external energy. Internal energy maintains the smoothness in the deformation procedure and external energy converge the model in the direction of the contour of the organism. The active contour model can be described as a set of n points in the image region $V = \{v_1, v_n\}$, $v_i = (x_i, y_i)$, $i = \{1, \ldots, n\}$. The boundary of the object is obtained by the iterative processing of the points on the initial contour [40]. An energy function in (1) for every point in the surrounding of v_i can be defined as:

$$E_{snake}(\mathrm{V}) = E_{int}(\mathrm{V}) + \beta \mathrm{E}_{\mathrm{ext}}(\mathrm{V}) \tag{1}$$

The energy function E_{int} *(V)* rely on the structure of the boundary whereas the energy function E_{ext}*(V)* rely on the characteristics of the ultrasound image like gradient adjacent to point v_i. The β is the constant, which gives the comparative weighting of the energy functions. The middle point in each of the matrices E_{ext}, E_{snake}, and E_{int} represents the energy at location v_i. Every location v_i moves to the new location v_i' based on the point of the lowest value in E_{snake}*(V)*. When the energy terms are opted perfectly, then the boundary '*V*' proceed towards the target tissue boundary and stops when actual object boundary is obtained.

Tony et al. [58] proposed active contour based segmentation using curve evolution, without image gradient information. This technique detected the contour of different shapes in an automated way when tested on extremely noisy synthetic image. Objects with smooth boundaries or not having gradient information were segmented successfully and therefore, can be tested on TRUS images for prostate segmentation where the gradient information is very less especially at the base and apex region.

TRUS contains large number of edge features which are not the part of prostate contour and low SNR. Therefore, conventional active contour model may not be able to deform the boundary to the accurate prostate contour. Hence, Yanyan et al. [71] used the combination of conventional active contour model and region based energy. Region based energy is helpful for contouring the prostate because the pixel inside the prostate are darker than the background. The mean absolute distance (MAD) and area overlap of $0{,}85 \pm 0.19$ mm and $91.3 \pm 3.09\%$ respectively, was obtained when tested on 336 2D TRUS images acquired from 15 patients. Instead of using traditional intensity priors and statistical models of shape [58,72], Soumya et al. [73] built multiple mean parametric model using posterior probabilities of the prostate region. The proposed technique obtained DSC and MAD of 0.97 ± 0.01 and 0.49 ± 0.20 mm respectively, when tested on 23 datasets. However, the proposed technique was validated only on the central gland TRUS images. Later, this work [73] was extended by Soumya et al. [74] by validating a new active appearance model on 46 mid, 40 base and 40 apex region of prostate in TRUS images. The proposed technique obtained DCS of 0.91 ± 0.09 with segmentation time of 0.67 ± 0.02 s. The use of intensities with posteriors has significantly improved the accuracy of segmentation in contrast with active appearance model [58,72].

3.2.2. Level set models or geometric deformable models

The main drawback of active contour models in delineation of prostate in 3D ultrasound images is the difficulty of tackling structural modifications for separating and merging of boundaries [63]. Level sets methods solve these structural modification issues. The interface is implicitly represented in level set approach. We represented the interface by Γ and level set function by ϕ. Initially Γ defines the level set zero $\{\phi = 0\}$. The characteristics of the function described across the image area is given by

$$\phi(x, y, t = 0) = \pm d(x, y) \tag{2}$$

In this, the term d is the distance between (x, y) and $\Gamma(t = 0)$, and the $\pm$ sign is used to describe whether the coordinates (x, y) lie in exterior or interior to the initial interface. If F denotes the speed with which the surface ϕ proceeds towards usual direction then, it can be described as:

$$\frac{\partial \varphi}{\partial t} + F|\nabla \phi| = 0 \quad \text{Given} \quad \phi(x, y, t = 0) \tag{3}$$

And the moving front at various point of time in zero level set is:

$$\Gamma(t) = \{(x, y) | \phi(x, y, t) = 0\} \quad (4)$$

The level set approach was originally introduced by Malladi et al. [55], since then many advancement in level set approaches have been introduced. Pengfei et al. [52] fine tuned the segmentation by a new level set model, which utilizes the combination of shape prior and contrast information. The proposed approach is appropriate for segmentation of apex, base and mid gland region of the prostate. The MAD of 1.40 ± 0.60, 1.74 ± 0.90 and 1.25 ± 0.77 is obtained for apex, base and mid gland region respectively when tested on 116 apex, 156 base and 194 mid gland TRUS images.

Tsai et al. [54] proposed a shape-based technique to curve evolution for contouring of medical images containing known object types. The resulting algorithm is able to handle multidimensional data, topological changes of the curve, and robust to noise. However, the distance functions utilized to define the shapes are not closed under linear operations; this gives rise to an inconsistent framework for shape modeling. Gong et al. [56] extended the work presented in [54] by embedding the shape descriptors in a region based level set approach for prostate ultrasound images. Authors [56] developed a hybrid level set segmentation approach using shape model estimation and curve evolution. This approach is less dependent on the initialization, robust to artifacts due to large calcification and yielded a mean absolute distance of 0.86 when tested on 4 ultrasound images. Rousson et al. [57] proposed a level set segmentation using Bayesian interface. Kernel density is calculated for the training data. The intensity information from 21 manually contoured ultrasound images is utilized using probabilistic model, and 92% of pixels are correctly classified.

Zhan et al. [41] used Gabor filter bank to extract the features from 45 3D TRUS images and mean voxel distance of 1.12 ± 0.15 is obtained. Gabor filter helps in boundary detection as its imaginary part can act as an edge detector and the real part work as a smoothening filter. Li et al. [61] proposed an active band to cope with intensity variation and edge descriptor to capture the weak contours in ultrasound image. This level set based technique is tested on 13 3D TRUS images, DSC of $94.87\% \pm 1.50\%$ and sensitivity of $93.16\% \pm 2.30\%$ is obtained. When same algorithm using100 2D TRUS images DSC and sensitivity of $95.82\% \pm 2.23\%$ and $94.87\% \pm 1.85\%$ respectively are obtained.

3.3. Semi-automated and fully-automated segmentation approaches

In semi-automatic prostate region contouring, the involvement of a radiologist or an expert is usually required to initialize the segmentation process or sometimes to correct the final segmentation result. A lot of research has been reported for semiautomatic segmentation [40,45–47], of prostate in order to reduce the human involvement as much as possible. Shenet al. [40] proposed an algorithm based on Gabor filter bank which required manual editing from human after edges are obtained in an automated way. Pathak et al. [45] used automatically detected boundary points as edge guidance for outlining the prostate. Gong et al. [46] proposed parametric shape modeling which requires more than 2 points to be specified by the user for its initialization. Tutar et al. [47] proposed a semiautomatic approach for prostate segmentation using spherical harmonics, which also requires human based initialization. Any approach, which requires human interaction either for initialization or manual editing after the final outcome has obtained, can be classified in semi-automated category.

In a completely automatic segmentation approaches [17,34,36,41,43,48–53] there is no human involvement in the process. These approaches often use model-based techniques like deformable model with superellipse or with any other prior knowledge of shape. However, the development of perfect automated approach is a difficult task due to acoustic shadowing and calcification in TRUS images. Some automated segmentation approaches [34,49] provided promising results with few milliseconds of processing time. Yan [34] executed the delineation process in a multi resolution way i.e. the boundary points of the seed model move to find the dark to light intensity variation. This technique improved the computational efficiency and robustness in an automated segmentation process.

3.4. Model-based image segmentation techniques advantages and limitations

Poor contrast, artifacts, and low SNR in TRUS images lead to missing edges and the contour of the prostate cannot be determined from local information as region homogeneity only. Expert radiologists are still able to segment the prostate due to the walnut shape of prostate gland in TRUS images. So experts have a priori information about the shape and appearance of the prostate. Model-based contouring techniques embed this knowledge into computer algorithms which have this prior information about the appearance and shape of the prostate. Advantages and limitations of various model-based segmentation approaches are discussed in the following points:

1) The primary advantage of active contour models [58,62] is that depending on the pre specified number of control parameters their convergence is usually fast. However, these models are dependent on the topological structure. Moreover, if image contains multiple region of interest, then multiple models need to be initialized, one for each region of interest.

2) The geometric deformation models [54,55] utilize a distance transformation to specify the structure from n dimensional to $(n+1)$ dimensional domain. In this, $n=1$ denotes curves, $n=2$ indicates the surfaces on the plane etc. The main advantage of such models is their ability to specify a structure in a domain with dimensionality same as the dataset space. For example, for two dimensional segmentation, a curve is transformed into a two dimensional surface. However, their dependence on gradient information makes deformable models sensitive to noise.

3) In contrast with conventional deformable models which follow deterministic energy minimization techniques, learning based classification techniques depend on probabilistic solution in which they maximize the probability [17]. Prior intensity shape based models [75,76] are not suitable for clinical target volume (CTV) and planning target volume (PTV) delineation. However, learning based multi-label segmentation technique [17] is also applicable in segmentation of clinical target volume and planning target volume for prostate brachytherapy using TRUS images.

4. Validation metrics

The performance measures used to validate the segmentation process can be classified into *two* major categories. Distance based and volume based metrics. These metrics are used to express the variability between the manual and automatic generated contours of the prostate.

4.1. Distance based metrics

Usually we define the metric $m(A, B)$ as the difference among the two boundaries, described by sets of locations, $R = (r_1, r_2, \ldots r_m)$ and $S = (s_1, s_2, \ldots s_n)$. Every r_i and s_j is a point at the respective boundary. The distance of the nearest point (DNP) from r_i to s_j can be define as $d(ri, S) = min_j \|s_j - r_i\|$, with $\|\cdot\|$ represents the 2D Euclidean distance between any two arbitrary points. Similarly,

Table 1
Summary of prostate segmentation approaches in ultrasound images(Metrics are in mean±standard deviation format).

Year & Authors	Semi or Fully Automated Segmentation	Modality	Technique Used	Performance Evaluation					
				Distance-based metrics		Volume based metrics			Time needed to Segment a single image
				Hausdorff distance distance (eH) in mm	Mean absolute distance (eM) in mm	Overlap volume error(%)	Volume Error (%)	Average distance error (Voxels)	
1999 [36]	FA	77–2D TRUS	Multiscale contour parameterization based on the 1D dyadic wavelet transform	NA	NA	NA	10.97	NA	NA
2000 [45]	SA	125–2D TRUS	Antistropic Diffusion Filter with Canny's Edge detector	1.8 ± 1.0	0.7 ± 0.4	NA	NA	NA	With Pentium 233-MHz approx. 30 s
2003 [40]	SA	8–2D TRUS	Hierarchical Deformation strategy by using Gabor filter bank	NA	3.20 ± 0.87	NA	NA	NA	With 500-MHz processor, 64 s
2004 [46]	SA	125–2D TRUS	Deformable superellipses with Bayesian segmentation	1.32 ± 0.62	$0.54 \pm$n0.20	NA	NA	NA	With Pentium-4, 2 GHz approx. 5 s
2006 [41]	FA	6–3D TRUS	Shape statistics and texture priors using Gabor-support vector machine	NA	NA	4.16 ± 0.54	2.22 ± 1.19	1.12 ± 0.15	With 2.8G Xeon PC, 180 sec
2006 [47]	SA	30–3D TRUS	Shape constraints using Spherical Harmonics	NA	NA	83.5 ± 4.2	NA	1.26 ± 0.41	With 3- GHz Pentium4, 120 s
2007 [43]	FA	9–3D TRUS	Continuity constraints, Autoagressive model	NA	NA	NA	NA	1.87	With Pentium4 2.8 GHz, 10 s
2008 [48]	FA	22–2D TRUS	Multipopulation genetic algorithm	3.93 ± 1.90	1.65 ± 0.67	NA	NA	NA	With 2.0 GHz Xeon PC, 11 min
2010 [34]	FA	301–2D TRUS	DDM Shape priors with partail active shape model	NA	2.01 ± 1.02	NA	NA	NA	With Core2 1.86-GHz PC, 0.3 s
2011 [49]	FA	3064–2D TRUS	GPSS and ALSS	NA	1.65 ± 0.47	NA	NA	NA	With core2 1.86-GHz PC, 200 ms
2013 [50]	FA	132 2D TRUS	Intrinsic properties, non-parametric shape prior, Gabor filter banks	NA	1.21 ± 0.85	NA	NA	NA	With Intel2.4 GHz processor, 19 s
2014 [51]	FA	25–3D TRUS	CCMFM with Axial Symmetry prior	NA	NA	NA	2.4 ± 1.6	1.1 ± 0.3	With 4-core intel i7 3,4 GHz, 6S
2015 [52]	FA	Two 2D TRUS dataset with 132 & 150	Intrinsic properties, speckle size and orientations	3.59 ± 1.97 and 3.52 ± 1.96	1.06 ± 0.53 and 1.25 ± 0.77	NA	NA	NA	With Intel Core i5 2.4 GHz, 104 s
2015 [53]	FA	280 2D TRUS	Multi-atlas fusion framework	5.48 ± 1.71	1.77 ± 0.98	NA	10.25 ± 3.74	NA	Intel Core i7, 2.93 GHz, 163 s
2016 [17]	FA	590–2D TRUS	learning based Multi-label Segmentation	5.4 ± 1.38	0.98 ± 0.39	NA	9.95 ± 3.53	NA	With intel Core i7 2.93 GHz, 300 ms

FA: Fully Automated.
SA: Semi-Automated.
NA: Not Available.
GPSS: Global population based shape statistics.
ALSS: Adaptive local shape statistics.
TRUS: Transrectal Ultrasound.
DDM: Discrete Deformable Model.
CCMFM: Coherent continuous max-flow model.

Table 2
Segmentation techniques advantages and disadvantages.

	Segmentation Method	Advantages	Disadvantages
Model-based	Level Sets	Topological variations are possible with ease	Computational complexity is high, requires long processing time [41]
	Parametric Deformation Models (Active Contour)	Changes in shape over time can be easily accommodated [46]	TRUS contains heterogeneous intensity, hence model may result to the wrong boundaries
Region-based	Texture Analysis	Useful for segmenting the regions having similar texture variations	Variation in texture may results in holes and requires additional edge joining approaches to be followed [37]

we can define the distance between a point on boundary R and a point on boundary S. The Hausdorff distance distance (e_H) can be described as the maximum distance to the nearest point (DNP) among every point on two different boundaries. The e_H is the worst possible disagreement between two subsets of a metric space.

Mean absolute distance $(e_M)$is the average of DNPs between two boundaries.

4.2. Volume based metrics

Volume error *(VE)* in (5) can be described as the number of voxels between the automatically segmented volume *(ASV)* and manually segmented volume *(MSV)* of the gland. It can be calculated as [36]:

$$VE = [(MSV \cup ASV) - (MSV \cap ASV)]/2MSV \quad (5)$$

The overlap volumetric error *(OVE)* can be defined as

$$\boldsymbol{OVE} = 1 - \frac{|\boldsymbol{MSI} \cap \boldsymbol{ASI}|}{|\boldsymbol{MSI} \cup \boldsymbol{ASI}|} \quad (6)$$

Where *MSI* and *ASI* in (6) and (7), denote the manually segmented image and automated segmented image. $\bigcup$ And $\bigcap$ simply performs the *OR* and *AND* operations between voxels.

The relative volume difference *(RVD)* is used to verify if a result is over segmented or under segmented and is defines as [36]:

$$RVD = \frac{|ASI| - |MSI|}{MSI} \quad (7)$$

Other measures like Overlap ratio such as Jaccard and Dice are also used as validation metric and utilize ranges from 0 to 1. Here, 0 means, there is no spatial overlap between two boundaries and 1 indicates complete overlap. Although, there are numerous metrics to validate the segmentation results including area based metrics, the above stated are some of the most frequently used metrics and are presented from the view point of the performance comparison of different segmentation techniques reported in this survey. Further, to validate the segmentation results, manual contouring on clinical data by experts is used as the gold standard, with which auto generated contour can be compared. However, manual delineation as a reference suffers from the inter and intra-observer variability, which makes validation task difficult and the accuracy may be biased.

5. Critical analysis and discussion

The survey of the existing literature shows that the detection of prostate boundary from TRUS in an accurate, fast, and reproducible way is a challenging problem. A number of techniques for semi-automated and automated segmentation have been proposed. Although segmentation techniques based on local and global thresholding are simple and computationally fast, but have limited acceptability for TRUS prostate segmentation. However, thresholding based methods are used as the initial step in the segmentation process. Segmentation techniques developed in C++ based on MATLAB environment are found to be faster and have access time less than a second [18].

The comparison of existing state-of-the-art techniques for segmentation of prostate in TRUS image issummarized in Table 1. The advantages and disadvantages of various prostate segmentation techniques are presented in Table 2.

The semi-automated segmentation approaches [41,47] mentioned in Table 1 provided promising results, but fully automated approaches are more desirable. Two [52,53] fully automated segmentation approaches have provided good results with more processing time. Few researches [17,34,49] are able to perform completely automated segmentation with processing time requirement of less than 1 s per image, however the volumetric error is very high [17]. Volumetric estimations are helpful in grading of prostate cancer and various surgical tasks. Also, the segmentation time plays an important role asmost of the clinical applications and surgeries are time bounded. As mentioned in Table 2, with level set approach topological variations are possible with ease, however computational complexity is high and requires long processing time [41]. Variation in shape can be accommodated with parametric deformation models [46] but due to heterogeneous intensity variation in TRUS wrong boundaries can be identified. The texture analysis segmentation approaches are helpful to segment the regions with similar texture variation and may require additional edge joining procedure to be followed [37]. However, to deal with heterogeneous texture variation, Gabor support vector machines can be positioned locally on patches of TRUS image [41]. This can adaptively capture the texture information near prostate and non-prostate region especially at base and apex of prostate where the texture variations are large, having low SNR value. The comparison of the performance of several existing prostate segmentation approaches can be best analyzed by testing them on standard dataset. However, there is no standard dataset available on TRUS images.

6. Conclusion and future trend

Detecting the prostate boundary from TRUS in a fast, accurate, and reproducible way is a challenging problem. The need for accurate automated prostate segmentation technique in TRUS images is increasing day by day as number of modern clinical applications like brachytherapy, volume estimation, localization of cancerous region and biopsy needle placement are heavily dependent on the accurate prostate delineation. Region based approaches for prostate delineation is primarily used to refine the obtained connected boundary [35–38]. Few region-based approaches [40] yield promising results, but require human interventions. Thresholding based approaches are fast and simple but usually used as initial step in the contouring process. Model based approaches are widely accepted due to their high sensitivity in finding the contour of prostate gland. Level sets or deformation models can help in development of accurate and completely automated segmentation for prostate delineation [61]. As these methods are time very time consuming [48], so graphic processing unit based programming can be used to support the real-time biopsy process. Few learning based multi labeled approaches [17] are very fast (execution time is in millisecond), as the proposed methodology is not iterative. In future, it is crucial to address the contouring process towards completely automated segmentation. This requires embedding human intelligence in algorithms, prior information about intensity variation, and structural details

(shape and size) of the prostate gland. The existing convolutional neural networks require significantly large datasets to produce the good results for localization and object identification task. However, it is difficult and also expensive to get large datasets. Thus, in future deep learning methods with deep network topologies need to be used to obtain admirable results in the segmentation of prostrate region in short duration. However, unsupervised completely automatic segmentation approaches are desirable.

All the studies reported in this paper concern TRUS imaging. TRUS images are quite appropriate for cancer screening, TRUS-guided biopsies and for prostate shape estimation. But, it is difficult to use TRUS imaging routinely for localization during successive radiotherapy sequences. Moreover, TRUS is invasive and uncomfortable imaging test. The trans-abdominal imaging is more suitable to intra-operative environment and intra-treatment visualization than the TRUS imaging [70]. Therefore, there is a need to work on prostate segmentation using abdomen ultrasound images as these images are taken non-invasively and commonly used modality for prostate diagnosis as compared to TRUS, which is invasive.

Acknowledgement

This research is funded under Junior Research Fellowship (JRF) scheme by the University Grant Commission (UGC), New Delhi, India.

References

[1] American cancer society. Prostate cancer statistics http://www.cancer.org/cancer/prostatecancer/detailedguide/prostate-cancer-key-statistics (Accessed 28 March 2017).
[2] Gyan Pareek, U. Rajendra Acharya, S. Vinitha Sree, G. Swapna, Ratna Yantri, Roshan Joy Martis, Luca Saba, et al., Prostate tissue characterization/classification in 144 patient population using wavelet and higher order spectra features from transrectal ultrasound images, Technol. Cancer Res. Treat. 12 (6) (2013) 545–557.
[3] Joe Philip, Subhajit Dutta Roy, Mohammed Ballal, Christopher S. Foster, Pradip Javlé, Is a digital rectal examination necessary in the diagnosis and clinical staging of early prostate cancer? BJU Int. 95 (7) (2005) 969–971.
[4] Richard M. Hoffman, Frank D. Gilliland, Meg Adams-Cameron, William C. Hunt, R. Key. Charles, Prostate-specific antigen testing accuracy in community practice, BMC Fam. Practice 3 (1) (2002) 19.
[5] Maarten de Rooij, Esther H.J. Hamoen, J. Alfred Witjes, Jelle O. Barentsz, Maroeska M. Rovers, Accuracy of magnetic resonance imaging for local staging of prostate cancer: a diagnostic meta-analysis, Eur. Urol. 70 (2) (2016) 233–245.
[6] S.D. Heenan, Magnetic resonance imaging in prostate cancer, Prostate Cancer Prostatic Dis. 7 (4) (2004) 282–288.
[7] O. Basset, Z. Sun, J.L. Mestas, G. Gimenez, Texture analysis of ultrasonic images of the prostate by means of co-occurrence matrices, Ultrasonic Imaging 15 (3) (1993) 218–237.
[8] A.L. Huynen, R.J.B. Giesen, J.J.M.C.H. De La Rosette, R.G. Aarnink, F.M.J. Debruyne, H. Wijkstra, Analysis of ultrasonographic prostate images for the detection of prostatic carcinoma: the automated urologic diagnostic expert system, Ultrasound Med. Biol. 20 (1) (1994) 1–10.
[9] A. Houston, S.B. Prem kumar Glen, David E. Pitts, R.J. Babaian, Prostate ultrasound image analysis: localization of cancer lesions to assist biopsy, in: Computer-Based Medical Systems, 1995, Proceedings of the Eighth IEEE Symposium on, IEEE, 1995, pp. 94–101.
[10] G. Schmitz, H. Ermert, Th Senge, Tissue-characterization of the prostate using radio frequency ultrasonic signals, IEEE Trans. Ultrason. Ferroelectr. Freq. Control 46 (1) (1999) 126–138.
[11] Ulrich Scheipers, Helmut Ermert, Hans-Joerg Sommerfeld, Miguel Garcia-Schürmann, Theodor Senge, Stathis Philippou, Ultrasonic multifeature tissue characterization for prostate diagnostics, Ultrasound Med. Biol. 29 (8) (2003) 1137–1149.
[12] Elizabeth P. Ives, Melissa A. Burke, Pamela R. Edmonds, Leonard G. Gomella, Ethan J. Halpern, Quantitative computed tomography perfusion of prostate cancer: correlation with whole-mount pathology, Clin. Prostate Cancer 4 (2) (2005) 109–112.
[13] René G. Aarnink, Sayan Dev Pathak, Jean J.M.C.H. De La Rosette, Frans M.J. Debruyne, Yongmin Kim, Hessel Wijkstra, Edge detection in prostatic ultrasound images using integrated edge maps, Ultrasonics 36 (1-5) (1998) 635–642.
[14] W. James Morris, Mira Keyes, Ingrid Spadinger, Winkle Kwan, Mitchell Liu, Michael McKenzie, Howard Pai, Tom Pickles, Scott Tyldesley, Population-based 10-year oncologic outcomes after low-dose-rate brachytherapy for low-risk and intermediate-risk prostate cancer, Cancer 119 (8) (2013) 1537–1546.
[15] S. Bridal, J.-M. Lori, Amena Saied Correas, Pascal Laugier, Milestones on the road to higher resolution, quantitative, and functional ultrasonic imaging, Proc. IEEE 91 (10) (2003) 1543–1561.
[16] S. Mahdavi, Nick Chng Sara, Ingrid Spadinger, William J. Morris, E. Septimiu, Salcudean Semi-automatic segmentation for prostate interventions, Med. Image Analysis 15 (2) (2011) 226–237.
[17] Saman Nouranian, Mahdi Ramezani, Ingrid Spadinger, William J. Morris, Septimu E. Salcudean, Purang Abolmaesumi, Learning-based multi-label segmentation of transrectal ultrasound images for prostate brachytherapy, IEEE Trans. Med. Imaging 35 (3) (2016) 921–932.
[18] Ernest J. Feleppa, Christopher R. Porter, Jeffrey Ketterling, Paul Lee, Shreedevi Dasgupta, Stella Urban, Andrew Kalisz, Recent developments in tissue-type imaging (TTI) for planning and monitoring treatment of prostate cancer, Ultrason. Imaging 26 (3) (2004) 163–172.
[19] Soumya Ghose, Arnau Oliver, Robert Martí, Xavier Lladó, Joan C. Vilanova, Jordi Freixenet, Jhimli Mitra, Désiré Sidibé, Fabrice Meriaudeau, A survey of prostate segmentation methodologies in ultrasound, magnetic resonance and computed tomography images, Comput. Methods Programs Biomed. 108 (1) (2012) 262–287.
[20] J. Alison Noble, Djamal Boukerroui, Ultrasound image segmentation: a survey, IEEE Trans. Med. Imaging 25 (8) (2006) 987–1010.
[21] Yanong Zhu, Stuart Williams, Reyer Zwiggelaar, Computer technology in detection and staging of prostate carcinoma: a review, Med. Image Anal. 10 (2) (2006) 178–199.
[22] Fan Shao, Keck Voon Ling, Wan Sing Ng, Ruo Yun Wu, Prostate boundary detection from ultrasonographic images, J. Ultrasound Med. 22 (6) (2003) 605–623.
[23] Richard N. Czerwinski, Douglas L. Jones, W.D. O'Brien, Edge detection in ultrasound speckle noise, IEEE, in: Image Processing, 1994. Proceedings. ICIP-94., IEEE International Conference, vol. 3, 1994, pp. 304–308.
[24] Galen C. Hunt, Randal C. Nelson, Lineal feature extraction by parallel stick growing, in: International Workshop on Parallel Algorithms for Irregularly Structured Problems, Springer, Berlin, Heidelberg, 1996, pp. 171–182.
[25] Sayan D. Pathak, Peter D. Grimm, Vikram Chalana, Yongmin Kim, Pubic arch detection in transrectal ultrasound guided prostate cancer therapy, IEEE Trans. Med. Imaging 17 (5) (1998) 762–771.
[26] Christian J. Knoll, Mariano L. Alcaniz-Raya, Carlos Monserrat, Vincente Grau Colomer, M. Carmen Juan, Multiresolution segmentation of medical images using shape-restricted snakes, in: Medical Imaging'99, International Society for Optics and Photonics, 1999, pp. 222–233.
[27] Savita Gupta, L. Kaur, R.C. Chauhan, S.C. Saxena, A wavelet based statistical approach for speckle reduction in medical ultrasound images, IEEE, in: TENCON 2003. Conference on Convergent Technologies for the Asia-Pacific Region, vol. 2, 2003, pp. 534–537.
[28] S. Gupta, R.C. Chauhan, S.C. Saxena, Locally adaptive wavelet domain Bayesian processor for denoising medical ultrasound images using speckle modelling based on Rayleigh distribution, IEE Proc. Vis. Image Signal Process. 152 (1) (2005) 129–135.
[29] S. Gupta, R.C. Chauhan, S.C. Saxena, Homomorphic wavelet thresholding technique for denoising medical ultrasound images, J. Med. Eng. Technol. 29 (5) (2005) 208–214.
[30] U. Acharya, Rajendra S. Vinitha Sree, G. Swapna, Savita Gupta, Filippo Molinari, R. Garberoglio, Agnieszka Witkowska, Jasjit S. Suri, Effect of complex wavelet transform filter on thyroid tumor classification in three-dimensional ultrasound, Proc. Inst. Mech. Eng. H 227 (3) (2013) 284–292.
[31] Savita Gupta, Lakhwinder Kaur, R.C. Chauhan, S.C. Saxena, A versatile technique for visual enhancement of medical ultrasound images, Digital Signal Process. 17 (3) (2007) 542–560.
[32] R.G. Aarnink, R.J.B. Giesen, A.L. Huynen, J.J.M.C.H. De La Rosette, F.M.J. Debruyne, H. Wijkstra, A practical clinical method for contour determination in ultrasonographic prostate images, Ultrasound Med. Biol. 20 (8) (1994) 705–717.
[33] C.H. Chen, J.Y. Lee, W.H. Yang, C.M. Chang, Y.N. Sun, Segmentation and reconstruction of prostate from transrectal ultrasound images, Biomed. Eng. Appl. Basis Commun. 8 (1996) 287–292.
[34] Pingkun Yan, Sheng Xu, Baris Turkbey, Jochen Kruecker, Discrete deformable model guided by partial activeshape model for TRUS image segmentation, IEEE Trans. Biomed. Eng. 57 (5) (2010) 1158–1166.
[35] William D. Richard, Constance G. Keen, Automated texture-based segmentation of ultrasound images of the prostate, Comput. Med. Imaging Graph. 20 (3) (1996) 131–140.
[36] Christian Knoll, Mariano Alcañiz, Vicente Grau, Carlos Monserrat, M. Carmen Juan, Outlining of the prostate using snakes with shape restrictions based on the wavelet transform (Doctoral Thesis: Dissertation), Pattern Recognit. 32 (10) (1999) 1767–1781.
[37] Hanif M. Ladak, Fei Mao, Yunqiu Wang, Dónal B. Downey, David A. Steinman, Aaron Fenster, Prostate boundary segmentation from 2D ultrasound images, Med. Phys. 27 (8) (2000) 1777–1788.
[38] Yunqiu Wang, H. Neale Cardinal, Donal B. Downey, Aaron Fenster, Semiautomatic three-dimensional segmentation of the prostate using two-dimensional ultrasound images, Med. Phys. 30 (5) (2003) 887–897.
[39] Purang Abolmaesumi, Mohammad Reza Sirouspou, An interacting multiple model probabilistic data association filter for cavity boundary extraction from ultrasound images, IEEE Trans. Med. Imaging 23 (6) (2004) 772–784.

[40] Dinggang Shen, Yiqiang Zhan, Christos Davatzikos, Segmentation of prostate boundaries from ultrasound images using statistical shape model, IEEE Trans. Med. Imaging 22 (4) (2003) 539–551.
[41] Yiqiang Zhan, Dinggang Shen, Deformable segmentation of 3-D ultrasound prostate images using statistical texture matching method, IEEE Trans. Med. Imaging 25 (3) (2006) 256–272.
[42] N.N. Kachouie, P. Fieguth, A medical texture local binary pattern for TRUS prostate segmentation, in: Engineering in Medicine and Biology Society, 2007, EMBS 2007. 29th Annual International Conference of the IEEE, IEEE, 2007, pp. 5605–5608.
[43] Mingyue Ding, Bernard Chiu, Igor Gyacskov, Xiaping Yuan, Maria Drangova, Dònal B. Downey, Aaron Fenster, Fast prostate segmentation in 3D TRUS images based on continuity constraint using an autoregressive model, Med. Phys. 34 (11) (2007) 4109–4125.
[44] Soumya Ghose, Arnau Oliver, Robert Marti, Xavier Lladó, Jordi Freixenet, Joan C. Vilanova, Fabrice Meriaudeau, Prostate segmentation with local binary patterns guided active appearance models, in: SPIE Medical Imaging, International Society for Optics and Photonics, 2011, p. 796218.
[45] S.D. Pathak, D.R. Haynor, Y. Kim, Edge-guided boundary delineation in prostate ultrasound images, IEEE Trans. Med. Imaging 19 (12) (2000) 1211–1219.
[46] Lixin Gong, Sayan D. Pathak, David R. Haynor, Paul S. Cho, Kim. Yongmin, Parametric shape modeling using deformable superellipses for prostate segmentation, IEEE Trans. Med. Imaging 23 (3) (2004) 340–349.
[47] Ismail B. Tutar, Sayan D. Pathak, Lixin Gong, Paul S. Cho, Kent Wallner, Yongmin Kim, Semiautomatic 3-D prostate segmentation from TRUS images using spherical harmonics, IEEE Trans. Med. Imaging 25 (12) (2006) 1645–1654.
[48] F. Cosío, Arámbula Automatic initialization of an active shape model of the prostate, Med. Image Anal. 12 (4) (2008) 469–483.
[49] Pingkun Yan, Sheng Xu, Baris Turkbey, Jochen Kruecker, Adaptively learning local shape statistics for prostate segmentation in ultrasound, IEEE Trans. Biomed. Eng. 58 (3) (2011) 633–641.
[50] Pengfei Wu, Yiguang Liu, Yongzhong Li, Yongtao Shi, TRUS image segmentation with non-parametric kernel density estimation shape prior, Biomed. Signal Process. Control 8 (6) (2013) 764–771.
[51] Wu Qiu, Jing Yuan, Eranga Ukwatta, Yue Sun, Martin Rajchl, Aaron Fenster, Prostate segmentation: an efficient convex optimization approach with axial symmetry using 3-D TRUS and MR images, IEEE Trans. Med. Imaging 33 (4) (2014) 947–960.
[52] Pengfei Wu, Yiguang Liu, Yongzhong Li, Bingbing Liu, Robust prostate segmentation using intrinsic properties of trus images, IEEE Trans. Med. Imaging 34 (6) (2015) 1321–1335.
[53] Saman Nouranian, S. Sara Mahdavi, Ingrid Spadinger, William J. Morris, Septimu E. Salcudean, Purang Abolmaesumi, A multi-atlas-based segmentation framework for prostate brachytherapy, IEEE Trans. Med. Imaging 34 (4) (2015) 950–961.
[54] Andy Tsai, Anthony Yezzi, William Wells, Clare Tempany, Dewey Tucker, Ayres Fan, W. Eric Grimson, Alan Willsky, A shape-based approach to the segmentation of medical imagery using level sets, Ieee Trans. Med. Imaging 22 (2) (2003) 137–154.
[55] Ravi Malladi, James A. Sethian, Baba C. Vemuri, Shape modeling with front propagation: a level set approach, IEEE Trans. Pattern Anal. Mach. Intell. 17 (2) (1995) 158–175.
[56] Lixin Gong, Lydia Ng, Sayan D. Pathak, Ismail Tutar, Paul S. Cho, David R. Haynor, Yongmin Kim, Prostate ultrasound image segmentation using level set-based region flow with shape guidance, in: Medical Imaging, International Society for Optics and Photonics, 2005, pp. 1648–1657.
[57] Mikael Rousson, Daniel Cremers, Efficient kernel density estimation of shape and intensity priors for level set segmentation, in: International Conference on Medical Image Computing and Computer-Assisted Intervention, Springer, Berlin, Heidelberg, 2005, pp. 757–764.
[58] T.F. Chan, L.A. Vese, Active contours without edges, IEEE Trans. Image Process. 10 (2) (2001) 266–277.
[59] Laurent Saroul, Olivier Bernard, Didier Vray, Denis Friboulet, Prostate segmentation in echographic images: a variational approach using deformable super-ellipse and Rayleigh distribution, in: Biomedical Imaging: From Nano to Macro, 2008. ISBI 2008. 5th IEEE International Symposium on, IEEE, 2008, pp. 129–132.
[60] Alessandro Sarti, Cristiana Corsi, Elena Mazzini, Claudio Lamberti, Maximum likelihood segmentation of ultrasound images with Rayleigh distribution, IEEE Trans. Ultrason. Ferroelectr. Freq. Control 52 (6) (2005) 947–960.
[61] X. Li, C. Li, A. Fedorov, T. Kapur, X. Yang, Segmentation of prostate from ultrasound images using level sets on active band and intensity variation across edges, Med. Phys. 43 (6) (2016) 3090–3103.
[62] Michael Kass, Andrew Witkin, Demetri Terzopoulos, Snakes: active contour models, Int. J. Comput. Vis. 1 (4) (1988) 321–331.
[63] Stanley Osher, James A. Sethian, Fronts propagating with curvature-dependent speed: algorithms based on Hamilton-Jacobi formulations, J. Comput. Phys. 79 (1) (1988) 12–49.
[64] Deep Gupta, R.S. Anand, Barjeev Tyagi, Despeckling of ultrasound medical images using nonlinear adaptive anisotropic diffusion in nonsubsampledshearlet domain, Biomed. Signal Process. Control 14 (2014) 55–65.
[65] Deep Gupta, R.S. Anand, Barjeev Tyagi, Ripplet domain non-linear filtering for speckle reduction in ultrasound medical images, Biomed. Signal Process. Control 10 (2014) 79–91.
[66] Alin Achim, Anastasios Bezerianos, Panagiotis Tsakalides, Novel Bayesian multiscale method for speckle removal in medical ultrasound images, IEEE Trans. Med. Imaging 20 (8) (2001) 772–783.
[68] Ron Kohavi, A study of cross-validation and bootstrap for accuracy estimation and model selection, IJCAI 14 (2) (1995) 1137–1145.
[69] Timo Ojala, Matti Pietikainen, Topi Maenpaa, Multiresolution gray-scale and rotation invariant texture classification with local binary patterns, IEEE Trans. Pattern Anal. Mach. Intell. 24 (7) (2002) 971–987.
[70] Nacim Betrouni, Maximilien Vermandel, David Pasquier, Salah Maouche, Jean Rousseau, Segmentation of abdominal ultrasound images of the prostate using a priori information and an adapted noise filter, Comput. Med. Imaging Graph. 29 (1) (2005) 43–51.
[71] Yanyan Yu, Yimin Chen, Bernard Chiu, Fully automatic prostate segmentation from transrectal ultrasound images based on radial bas-relief initialization and slice-based propagation, Comput. Biol. Med. 74 (2016) 74–90.
[72] H. Burkhardt, B. Neumann, Active appearance models Proc. Eur. Conf. Computer Vision, vol. 2, Springer, 1998, 2017, pp. 484–498.
[73] Soumya Ghose, Arnau Oliver, Robert Martí, Xavier Lladó, Jordi Freixenet, Jhimli Mitra, Joan C. Vilanova, Josep Comet, Fabrice Meriaudeau, Multiple mean models of statistical shape and probability priors for automatic prostate segmentation, in: International Workshop on Prostate Cancer Imaging, Springer, Berlin Heidelberg, 2011, pp. 35–46.
[74] Soumya Ghose, Arnau Oliver, Jhimli Mitra, Robert Martí, Xavier Lladó, Jordi Freixenet, Désiré Sidibé, Joan C. Vilanova, Josep Comet, Fabrice Meriaudeau, A supervised learning framework of statistical shape and probability priors for automatic prostate segmentation in ultrasound images, Med. Image Anal. 17 (6) (2013) 587–600.
[75] Robert Toth, Justin Ribault, John Gentile, Dan Sperling, Anant Madabhushi, Simultaneous segmentation of prostatic zones using active appearance models with multiple coupled levelsets, Comput. Vis. Image Underst. 117 (9) (2013) 1051–1060.
[76] Jing Yang, James S. Duncan, 3D image segmentation of deformable objects with joint shape-intensity prior models using level sets, Med. Image Anal. 8 (3) (2004) 285–294.

R. P. Singh, received his B. Tech degree from SUSCET, PTU, Jalandhar (Punjab) in 2010, in Information Technology, and the M.Tech Degree from IGEF, PTU, Jalandhar (Punjab) in 2013, in Computer Science and Engineering. He is awarded with Junior Research Fellow (JRF) award from university grant commission (UGC), New Delhi in 2015. Currently, he is pursuing full time Ph.D in Computer Science and Engineering at *University Institute of Engg. & Technology*, *Panjab University*, Chandigarh. His research interests include Medical Image processing, segmentation and classification.

S. Gupta received her B.Tech. degree from TITS, Bhiwani (Haryana), in 1992, M.E. degree from TIET, Patiala, Punjab, in 1998 both in Computer Science and Engineering. She obtained her Ph.D. degree in 2007 in the field of Medical Ultrasound Image Processing. She has been into the teaching profession since 1992 and has published more than 90 papers in refereed International Journals and conference proceedings. Presently, she is working as Professor in the Department of CSE, *University Institute of Engg. & Technology, Panjab University*, Chandigarh. She has completed various research projects funded by various agencies like DST, AICTE and MHRD. Her research interests include *Medical image processing*, *Wavelets*, Neutrosophic logic, Network security, Wireless sensor networks and Cognitive Enhancement.

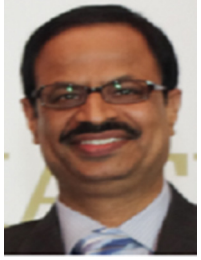

U. R. Acharya, PhD, DEng is a senior faculty member at Ngee Ann Polytechnic, Singapore. He is also (i) Adjunct Professor at University of Malaya, Malaysia, (ii) Adjunct Faculty at Singapore Institute of Technology- University of Glasgow, Singapore, and (iii) Associate faculty at SIM University, Singapore. He received his Ph.D. from National Institute of Technology Karnataka (Surathkal, India) and DEng from Chiba University (Japan). He has published more than 400 papers, in refereed international SCI-IF journals (345), international conference proceedings (42), books (17) with more than 11,500 citations in Google Scholar (with h-index of 55), and Research Gate RG Score of 45.00. He is ranked in the top 1% of the Highly Cited Researchers (2016) in Computer Science according to the Essential Science Indicators of Thomson. He has worked on various funded projects, with grants worth more than 2 million SGD. He has *three* patents and in the editorial board of many journals. He has served as guest editor for many journals. His major academic interests are in biomedical signal processing, biomedical imaging, data mining, visualization and biophysics for better healthcare design, delivery and therapy. Please visit https://scholar.google.com.sg/citations?user=8FjY99sAAAAJ&hl=en for more details.